HypIRskin: Thermography-Guided Device for Diagnosis and Characterization of Skin Cancer Lesions

Verstockt Jan
InViLab Research Group
University of Antwerp
Antwerp, Belgium
jan.verstockt@uantwerpen.be

Clarys Warre
InViLab Research Group
University of Antwerp
Antwerp, Belgium
0009-0002-5325-7750

Hillen Michaël
InViLab Research Group
University of Antwerp
Antwerp, Belgium
0000-0001-5859-8402

Verspeek Simon
InViLab Research Group
University of Antwerp
Antwerp, Belgium
0000-0002-4109-8839

Bonmarin Mathias
School of Engineering
Zurich University
of Applied Sciences
Winterthur, Switzerland
0000-0003-0227-9247

Thiessen Filip
Dept. of Plastic,
Reconstructive and Aesthetic Surgery
Antwerp University Hospital
Wilrijk, Belgium
0000-0002-4958-3150

Brochez Lieve
Dept. of Dermatology
Ghent University Hospital
Ghent, Belgium
0000-0001-6105-6719

Steenackers Gunther
InViLab Research Group
University of Antwerp
Antwerp, Belgium
0000-0001-9944-520X

***Abstract*—This paper presents the HypIRskin device, a functional prototype designed for the active thermography-based diagnosis and characterization of skin cancer lesions. The prototype's primary goal is to provide standardized and reproducible results within a clinical environment, thereby enhancing the efficiency of skin cancer diagnostics. The device, tested in a hospital setting, demonstrates rapid and efficient measurements, with a total time of approximately three minutes. Utilizing active infrared thermography, the device employs thermal excitation, specifically cooling the skin lesion, to capture its reheating pattern and rate. This approach takes advantage of heightened metabolic activity and angiogenesis associated with malignant cells, making it effective in characterizing skin cancers. The device integrates an infrared camera and an RGB camera, synchronized to capture simultaneous thermal and visual images of the same skin location during steady state, cooling and reheating. Results from cooling analyses using agar skin phantoms demonstrate the device's ability to provide uniform and reproducible cooling effects. The paper introduces the initial findings from testing the prototype on patients. It shows the captured images and thermal recovery curves of both affected and healthy skin areas. Additionally, it discusses the device's advantages, current research efforts, and future research, emphasizing its importance in dermatological diagnostics.**

***Index Terms*—Skin Cancer, Dynamic Infrared Thermography, Skin Cooling, Diagnosis, Skin Lesions**

This research was funded by the FWO via support for the FWO research project, "Optimized skin tissue identification by combined thermal and hyperspectral imaging methodology." (project number 41882 (FWO G0A9720N)). FWO-TBM (T001723N) - The use of dynamic infrared thermography for perforator mapping and quality improvement in autologous breast reconstructions. All subjects gave their informed consent for inclusion before they participated in the study. The study was conducted in accordance with the Declaration of Helsinki, and the protocol was approved by the Ethics Committee of the University Hospital Antwerp (B300201941125, date of approval: 16 May 2022).

I. Introduction

Cancer, a leading cause of premature death globally, claimed nearly 10 million lives in 2020, constituting almost one in six deaths. With over 19 million new cancer cases diagnosed in the same year, 1.50 million were attributed to skin cancer [1]. In Europe, rising incidences of melanoma and non-melanoma skin cancer are observed, particularly among elderly populations as a result of cumulative UV exposure. Incidence rates have tripled in Europe in the last four decades [2]. Early treatment of skin cancer is crucial to increase overall health. Conventional diagnostic methods like visual examination and biopsies have limitations [3]. Skin cancer screening often involves Total Body Skin Examination (TBSE) and dermoscopy, relying on the ABCDE classification for melanoma diagnosis [4]. Despite skilled dermatologists conducting these exams, specificity is relatively low, with moderate sensitivity [2]. This paper introduces a functional prototype, HypIRskin, for skin cancer characterization and diagnosis using dynamic infrared thermography. The prototype aims for standardized and reproducible results in a clinical setting.

A. Skin Cancer and Thermography

Active infrared thermography (IRT) for non-invasive skin temperature measurement utilizes infrared radiation in the long wave infrared range (LWIR: 8 (7.5)–14 μm). This technique involves intentional thermal excitation to enhance contrast, with its effectiveness in skin cancer detection demonstrated through cooling skin lesions to capture reheating patterns [5]. Active thermography, widely used in medical applications, is particularly adept at identifying skin cancer due to increased metabolic activity and angiogenesis in malignant cells [6]. Distinct thermal signatures in different skin tumor types allow

This text is the accepted manuscript of the following article: V. Jan et al., "HypIRskin: Thermography-Guided Device for Diagnosis and Characterization of Skin Cancer Lesions," 2024 IEEE International Symposium on Medical Measurements and Applications (MeMeA), Eindhoven, Netherlands, 2024, pp. 1-6, doi: 10.1109/MeMeA60663.2024.10596792.

thermography to differentiate between various skin cancers [7]. Thermal infrared imaging reveals blood vessel changes and chemical alterations linked to tumor development and growth [8]. Infrared thermography's advantage lies in discerning skin rewarming rates, enabling precise assessment of lesion boundaries and depth [9]. Notably, this technique avoids ionizing or harmful radiation, relying solely on the body's heat for imaging.

B. Related Work

State-of-the-art research, leveraging advancements in IR thermography and processing capabilities, offers novel insights into studying skin cancer. However, there is currently no standardized, reliable, quantitative, and non-invasive IRT-based method to accurately determine the malignant potential of skin lesions [5]. Previous studies employed various skin excitation methods, with common cooling methods including convection (cold air) or conduction (direct contact). Cooling with cold air from a vortex tube, fan, or air-conditioning unit, as well as conduction methods using cooled gel packs or aluminum medals, have been explored [5], [10]–[13]. Cameras were typically tripod-mounted in front of the lesion, while handheld IR devices were also employed to capture reheating patterns [5], [10], [12]. In steady state or after applying the cooling load, the entire skin surface has a homogeneous temperature, making it challenging to distinguish lesions from healthy skin. Researchers [5], [7], [10] addressed this by introducing a marker visible in both white light and thermographic images. The marker can also be used to compensate for patient movement and indicating the region of interest (ROI) to prevent errors during data acquisition with a macroscopic lens. Further insights into skin cancer diagnosis using infrared thermography can be found in the recent review by Verstockt et al. [14].

C. Creating reproducible results in a clinical setting

Ensuring the reproducibility and accuracy of results is vital for integrating the new technique into clinical settings and validating its application in medical infrared thermography. Continuous temperature monitoring during skin lesion cooling is essential, with convective cooling identified as the most suitable method for dermatologic applications due to its non-contact excitation. A recent study by Verstockt et al. [15] categorized six cooling methods into convection, conduction, and evaporative cooling. Results on a skin phantom favored convective cooling for its consistent and uniform effect, while conductive methods faced challenges with bulging or ulcerated lesions. The use of ice or alcohol was discouraged due to artifacts like a water layer or evaporated alcohol which obstructs the view. The Zimmer Cryo 6, a cryogenic cold air device, stood out among tested devices for its advantages, including uniform skin cooling, consistent cold air conditioning, high cooling efficiency at -30 °C, and compliance with medical device directives. Importantly, it did not obstruct the thermal camera's field of view, ensuring accurate recording of the skin lesion's cooling sequence. Its user-friendly nature contributed to reduced workload in clinical practice. For reproducible and accurate results, consistent measurement conditions, identical distances, angles relative to the skin and an uniform and constant application of cooling load are crucial. Recommendations from previous research include using macro lenses for enhanced resolution, careful camera positioning, and addressing patient motion correction, particularly with high-resolution macro images [14].

This innovative infrared thermography approach minimizes the need for complex surgical procedures, revealing previously undisclosed characteristics of skin lesions and aiding in more effective excisions. It reduces unnecessary excisions, promotes less invasive and economical treatment modalities, and contributes to improved aesthetic outcomes with smaller scars, enhancing patient safety and comfort.

II. Materials and Methods

A. Device Prototype

The device presented here is based on a previous unreported setup developed by Mathias Bonmarin at the Zurich University of Applied Sciences (ZHAW, Switzerland). The device is depicted in Figure 1. Its primary objective is to diagnose, characterize, and monitor skin diseases, with a particular emphasis on skin cancers. The initial focus is on characterizing the border and depth of skin lesions. Subsequently, the device's functionalities may be expanded to differentiate between malignant and benign lesions. The envisaged application of the device is in dermatological clinics or preceding surgical procedures, serving to determine the boundaries and depth of skin abnormalities.



Fig. 1. left: CAD model of the device, middle: CAD model of the internal structure of the device, right: Prototype device as built

1) Requirements: The established requirements offer flexibility for adapting the measurement protocol and device to meet validation needs. The device is made in such a way that it can be applied in a variety of clinical cases, therefore the requirements are not limited to fixed values. The non-restrictive specifications for the prototype are outlined as follows:

- The device must demonstrate ease of use and handling in a clinical setting.

- Measurements conducted by the device should exhibit accuracy and repeatability.
- The cooling excitation applied to the skin should be uniform and homogeneous and adhere to the physical constraints of the patient. The temperature and flow of the cold air should be adjustable, ensuring the device's readiness for research purposes.
- The device integrates an infrared camera operating in the long-wave infrared spectrum and an RGB camera for lesion tracking in the visual spectrum.
- The accompanying software is designed to be straightforward, requiring minimal expertise for operation.
- The device should be medical device directive compliant.

2) Hardware description: The design of the skin cancer diagnosis device utilizing active thermography adheres to the scheme outlined in Figure 2. The accompanying block diagram, presented in Figure 2, provides a comprehensive overview of the hardware components essential for the device's operation and illustrates the communication pathways between these components.

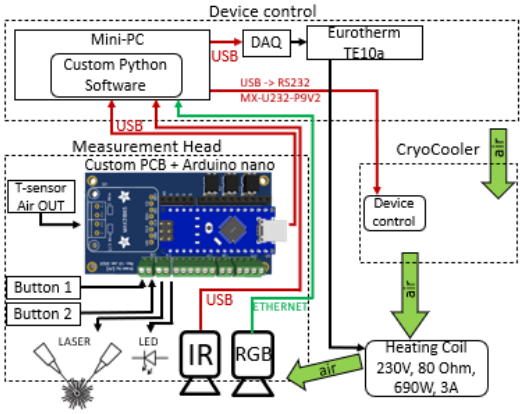


Fig. 2. Block diagram of the different hardware components of the device. The arrows represent the communication between components.

Main device body: At the core of the system lies a mini-PC, specifically the Udoo Bolt V8 featuring an embedded Quad-core processor, AMD Ryzen V1605B. This mini-PC operates with customized Python software, meticulously crafted to efficiently oversee and coordinate all hardware and software components in an intelligent, swift, and systematic manner (refer to paragraph II-A3 for details). The Zimmer Cryo C cooler is responsible for supplying conditioned dry air at a temperature of -30 °C. Control of the Cryo C cooler is facilitated through a custom Python library developed based on the Zimmer RS232 communication protocol. The USB to RS232 converter, mx-u232-p9v2 from Maxxtro, is employed for communicating with the Cryo C cooler.

Introducing a heating coil at the air output from the Cryo C enables the adjustment of air temperature. Powered by 230 VAC with 690 Watts of power, the heating coil can raise the air temperature from -30 °C to 60 °C. This dynamic temperature control capability even allows for the execution of lock-in thermography during device operation. The temperature of the air at the nozzle (5) output is monitored using a Platinum Thin Film Pt100 RTD resistor (6) with a fast thermal response time of 0.1s. The numbers between brackets correspond with the components in Figure 3. The measurement is facilitated by the Adafruit MAX31865 amplifier, specifically designed for precision temperature sensing applications, ensuring a total precision of at least 0.5 °C over all operating conditions. The Eurotherm TE10a, a Thyristor power controller, controls the operation of the heating coil. It receives a 4-20 mA signal from the National Instruments DAC (Digital-to-Analog Converter). The output signal of the DAC is calculated based on the set temperature and the actual temperature of the air at the nozzle. This control process is managed by a PID (Proportional-Integral-Derivative), programmed with a dedicated Python library, which regulates the output signal of the DAC to maintain precise temperature control.

Measurement head: The measurement head incorporates imaging devices, control elements, a temperature sensor (refer to paragraph II-A2), lasers, and LED arrays as shown in Figure 3. The different components are indicated with a number. The long-wave infrared camera used is the Optris Xi400 with microscope optics (1) (Optris GmbH, Berlin, Germany). This camera features an uncooled microbolometer detector with a pixel pitch of 17 μm and a thermal sensitivity (NETD) of $<$80 mK. Equipped with manual motor focus and microscope optics (AFOV: 18°$\times$14°), the thermal camera captures 16-bit RAW thermal image sequences at a resolution of 382 $\times$ 288 pixels and a frame rate of 27 Hz. The microscope optics enable close focusing on the subject, enhancing the visibility of minute details in skin lesions with high resolution. The Optris Xi400 has a focusing range spanning from 90 mm to 110 mm. A distance holder mounted to the measuring head maintains a consistent distance of 100 mm to the skin lesion.

The RGB camera (2) employed is the Daheng Imaging POE camera (MER-133-54GC-P) with a resolution of 1280 x 960 pixels with a polarizing filter to reduce reflections. Synchronized with the infrared camera, the RGB camera captures images simultaneously to facilitate movement compensation. The LED arrays (3) and laser positioning system are controlled with the Python software. The LED arrays use polarizing filters to illuminate the measurement area, minimizing reflections on the skin surface. The laser positioning system (4) consists of two red lasers (650 nm, 7 mW) positioned at an angle. When the measurement head is correctly positioned, the lasers converge to form a cross in the middle of the measurement area, simplifying the alignment above the skin lesion. Two buttons (8) are utilized for controlling the motorized focus of the thermal camera. Simultaneous pressing of both buttons initiates the measurement sequence (as described in section II-A3). A dedicated custom-made PCB (7) governs the operation of all hardware components within the measurement head. This specialized PCB incorporates the MAX31865 RTD-to-Digital Converter and an Arduino Nano (ATmega328 microcontroller). The Arduino Nano is linked to the mini-PC through serial communication. The microcontroller is

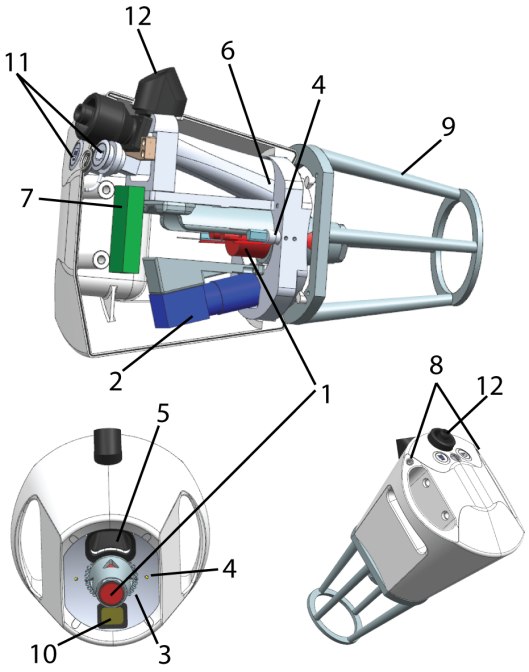


Fig. 3. CAD model of the measurement head with all components indicated. (1) Optris Xi400 (2) Daheng MER-133 (3) LED array (4) Laser (5) Nozzle outlet (6) PTF temperature sensor (7) Custom PCB (8) Buttons (9) Distance holder 100 mm (10) Polarizing window for RGB camera (11) USB and Ethernet connector (12) Mounting block

responsible for reading button states, toggling the LED and lasers, and managing temperature calculations and operates independently following an instruction set of a predefined algorithm.

3) Software description: The Python-written software for operating the active thermography skin cancer diagnosis device is designed with user-friendly features to ensure foolproof usage. The workflow, as illustrated in Figure 4, outlines the steps for utilizing the device. The software, responsible for camera control, utilizes the InViLab camera toolbox (GenPyCam, www.genpycam.com), which runs and manages all cameras. The UML class diagram depicted in Figure 5 showcases the structure of the HypIRskin software. Within this framework, the `ArduinoControl` class continuously monitors the Arduino's status, receives temperatures, manages button and LED/laser control. The `CentralControl` class orchestrates the collaboration of the DAC card, cameras, Arduino, cryocooler, and temperature control. The initiation of the measurement sequence is facilitated by the `start_measurement` method. During each measurement, `CentralControl` initiates the appropriate measurement type (steady state, cooling, or reheating) and waits on the signal that the measurement is complete. A dedicated .h5 file is generated for each measurement, storing parameters related to the measurement and patient, alongside image data, thermography parameters, and camera settings. The HypIRskin device is operated through a GUI featuring a main window, enabling comprehensive monitoring of all devices and facilitating measurement setup as can be seen in Figure 6. Once configured, the measurement sequence can be initiated directly from the main window.

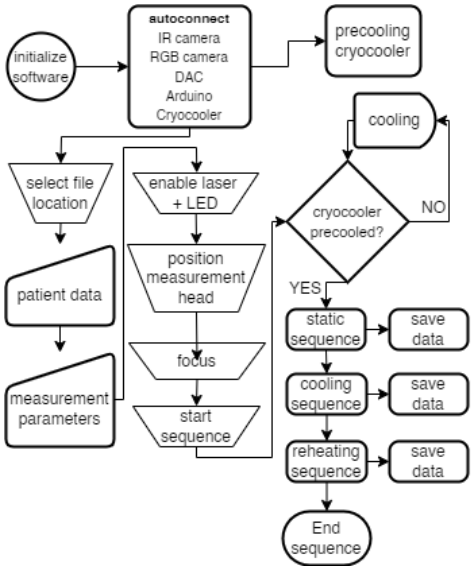


Fig. 4. Flow diagram of the software and usage of the device.

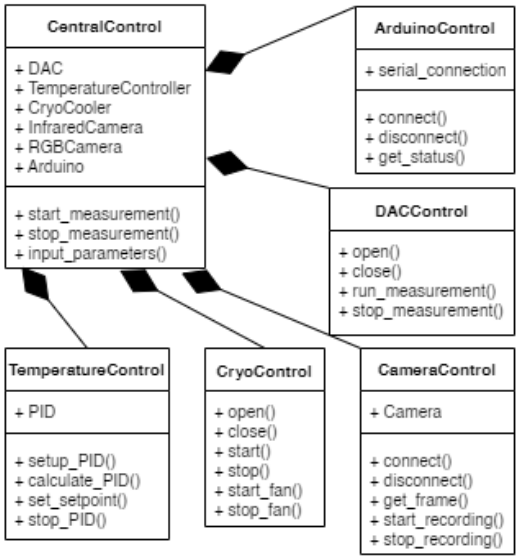


Fig. 5. UML class diagram for HypIRskin software. The camera object inherits from a custom made camera toolbox developed by the InViLab Research Group (GenPyCam, www.genpycam.com).

III. Results

A. Cooling Analysis

A comparative analysis of different cooling methods was carried out by the authors [15]. In this analysis, agarose skin phantoms are used to create a homogeneous and uniform material and to create reproducible results. The flat agar skin models were subjected to the cooling load of the cryogenic

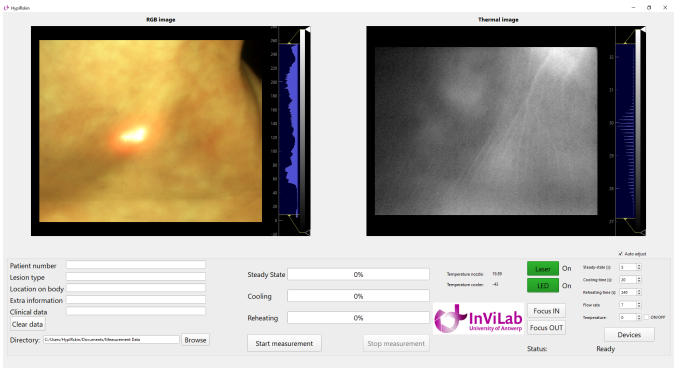


Fig. 6. GUI of the software to control the device. The left view is the RGB camera, the right view is from the thermal camera with a smaller field of view.

cooler at levels 1, 3 and 5 until the temperature of the skin phantom reached 15 °C at 5 mm depth. As depicted in Figure 7, level 5 demonstrates a more rapid cooling of the skin phantom compared to level 3 and level 1. Figure 8 illustrates the application of the device on the flat agar skin phantom and ulcerating skin phantom. The section of the skin phantom is shown at the top. The bulge has a diameter of 25 mm and a height of 5 mm. The thermograms selected at 5 s into the reheating are displayed. Below each thermogram, the corresponding histograms are shown. The histograms appear relatively narrow and tall, indicating uniform cooling distribution on the skin phantom.

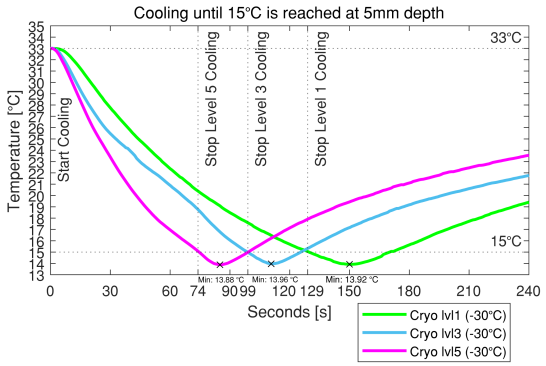


Fig. 7. The figure presents the results of applying three levels (1,3 and 5) of the cryo cooler on the flat agar skin phantom until the sample reached a temperature of 15 °C at 5 mm below the surface.

B. Prototype Test Results

The measurement head is positioned on the patient's skin, aligning it with the laser centered above the lesion. As of the current writing, data has been gathered from only five patients. Figure 9 provides an overview of the collected data at five seconds into the reheating sequence for a confirmed melanoma case. The top left image displays the RGB image with the red dot laser, while the adjacent image exhibits the corresponding infrared image in gray values. Within the software, the center of the lesion (red cross) is designated. The

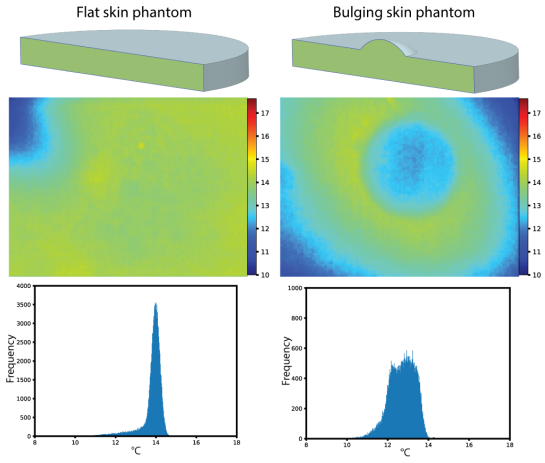


Fig. 8. top: Shape of the Agarose skin phantom, flat and ulcerating (bulging) skin lesion, middle: the results of the cryo cooling method. The circular area in the thermogram represents the ulcerating skin lesion, bottom: The Cryo cooler exhibits a uniform cooling pattern, as evident from the histograms.

point with the same temperature as the center of the lesion that is farthest from the lesion (blue cross) is identified, and for each point, the five nearest points with the same value are sought. The mean of these values is computed to mitigate measurement noise. In Figure 9, red crosses are positioned at the center of the melanoma, whereas blue crosses mark the healthy tissue region. The thermal recovery curve for both regions is depicted at the bottom of Figure 9. The maximum temperature difference between the healthy skin and malignant lesion is $\pm$ 0.8 °C. The temperature of the lesion increases more rapidly and reaches a higher level than that of the healthy skin, aligning with findings in the existing literature on this subject [5], [12].

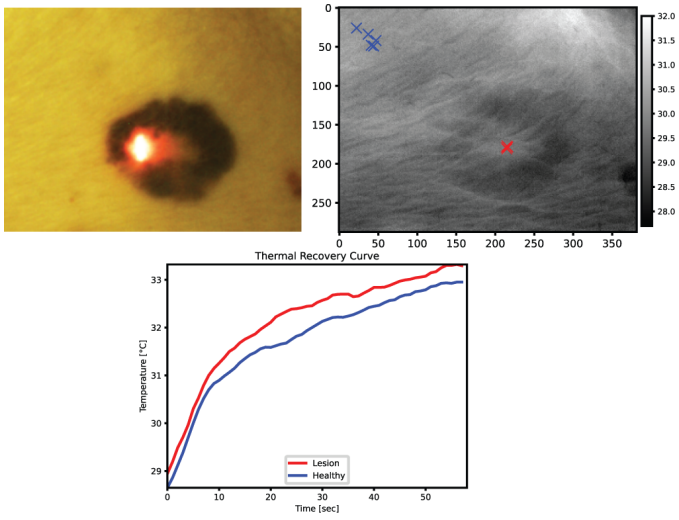


Fig. 9. Top left: RGB image of the lesion, Top right: corresponding thermogram with five points at the same temperature in center lesion (red) and healthy skin (blue), bottom: Thermal recovery curves of the red (lesion) points and the blue (healthy skin) points.

IV. Discussion and Conclusion

The successful application of the HypIRskin device in both clinical settings, namely at a doctor's practice and in a hospital environment, demonstrates its potential as an efficient tool for characterizing skin cancer using infrared thermography. The total measurement time of approximately three minutes showcases the device's rapidity, ensuring swift acquisition of crucial diagnostic information. The adjustable cooling load and duration offer flexibility in tailoring measurements to specific cases, indicating the potential for further optimization. The inclusion of laser guidance facilitates effortless device positioning, enhancing overall usability. However, the distance holder, while effective, is identified as an area for potential improvement in design to enhance user experience and streamline the setup process. The automation of the measurement protocol, not only contributes to time efficiency but also allows physicians to allocate their focus to other critical aspects of patient care. The homogeneous cooling load applied to the skin lesion proves advantageous, ensuring uniform and repeatable results. Standardizing the measurement cycle further enhances the efficiency of data processing, facilitating seamless integration into clinical workflows.

In conclusion, the cooling load administered (at level 5 of the cryo cooler) is effective in generating a temperature variance between the cancerous lesion and the adjacent skin during reheating. The extent of cooling penetration is adequate, yet further trials are necessary to refine the precise cooling load tailored to different body sites. Initial findings from this in-vivo device are promising, affirming the functionality of the technology and the developed device. Nonetheless, further investigation is warranted to determine the optimal device settings for achieving clinically significant outcomes.

V. Future Work

The ongoing research focuses on refining algorithms for automated lesion detection and accurately determining subcutaneous lesion depth and borders using thermographic data that will aid clinicians and dermatologists. Efforts are directed towards achieving a diagnostic distinction between benign and malignant lesions based on promising literature insights. Additional patient data needs to be acquired, necessitating the implementation of a measurement campaign to gather a substantial dataset. Future work includes efficiency updates for the control software and the development of a modular, adaptable distance holder. Further down the line, exploration into integrating multi- or hyperspectral imaging modalities into the measurement head is envisioned, offering a more comprehensive understanding of skin lesions. These advancements aim to enhance the HypIRskin device's diagnostic capabilities and position it as a versatile tool in dermatological diagnostics.

Acknowledgment

The successful design and construction of the active thermography device for skin cancer diagnosis would not have been possible without the invaluable support and collaboration of ZHAW and Prof. M. Bonmarin. Additionally, we extend our sincere gratitude to Prof. J. Lambert from the dermatology department of the Antwerp University Hospital for generously providing access to patients for the initial measurements.

References

[1] H. Sung, J. Ferlay, R. L. Siegel, M. Laversanne, I. Soerjomataram, A. Jemal, and F. Bray, "Global Cancer Statistics 2020: GLOBOCAN Estimates of Incidence and Mortality Worldwide for 36 Cancers in 185 Countries," *CA: A Cancer Journal for Clinicians*, vol. 71, no. 3, pp. 209–249, 2021. _eprint: https://onlinelibrary.wiley.com/doi/pdf/10.3322/caac.21660.

[2] A. Brunssen, A. Waldmann, N. Eisemann, and A. Katalinic, "Impact of skin cancer screening and secondary prevention campaigns on skin cancer incidence and mortality: A systematic review," *Journal of the American Academy of Dermatology*, vol. 76, pp. 129–139.e10, Jan. 2017. Publisher: Mosby Inc.

[3] N. Eisemann, A. Waldmann, A. C. Geller, M. A. Weinstock, B. Volkmer, R. Greinert, E. W. Breitbart, and A. Katalinic, "Non-Melanoma Skin Cancer Incidence and Impact of Skin Cancer Screening on Incidence," *Journal of Investigative Dermatology*, vol. 134, pp. 43–50, Jan. 2014.

[4] F. Nachbar, W. Stolz, T. Merkle, A. B. Cognetta, T. Vogt, M. Landthaler, P. Bilek, O. Braun-Falco, and G. Plewig, "The ABCD rule of dermatoscopy: High prospective value in the diagnosis of doubtful melanocytic skin lesions," *Journal of the American Academy of Dermatology*, vol. 30, pp. 551–559, Apr. 1994. Publisher: Elsevier.

[5] M. P. Çetingül, R. M. Alani, and C. Herman, "Quantitative Evaluation of Skin Lesions Using Transient Thermal Imaging," in *2010 14th International Heat Transfer Conference, Volume 1*, pp. 31–39, American Society of Mechanical Engineers Digital Collection, Mar. 2011.

[6] J. Flores-Sahagun, J. Vargas, and F. Mulinari-Brenner, "Analysis and diagnosis of basal cell carcinoma (BCC) via infrared imaging," *Infrared Physics & Technology*, vol. 54, pp. 367–378, Sept. 2011.

[7] T. M. Buzug, S. Schumann, L. Pfaffmann, U. Reinhold, and J. Ruhlmann, "Functional Infrared Imaging for Skin-Cancer Screening," in *2006 International Conference of the IEEE Engineering in Medicine and Biology Society*, pp. 2766–2769, Aug. 2006. ISSN: 1557-170X.

[8] A. M. N. Moustafa, H. H. Muhammed, and M. Hassan, "Skin Cancer Detection Using Temperature Variation Analysis," *Engineering*, vol. 05, no. 10, pp. 18–21, 2013.

[9] H. Chen, K. Wang, Z. Du, W. Liu, and Z. Liu, "Predicting the thermophysical properties of skin tumor based on the surface temperature and deep learning," *International Journal of Heat and Mass Transfer*, vol. 180, p. 121804, Dec. 2021.

[10] S. E. Godoy, M. M. Hayat, D. A. Ramirez, S. A. Myers, R. S. Padilla, and S. Krishna, "Detection theory for accurate and non-invasive skin cancer diagnosis using dynamic thermal imaging," *Biomedical Optics Express*, vol. 8, p. 2301, Apr. 2017.

[11] M. Bonmarin and F.-A. L. Gal, "A lock-in thermal imaging setup for dermatological applications," *Skin Research and Technology*, vol. 21, no. 3, pp. 284–290, 2015. _eprint: https://onlinelibrary.wiley.com/doi/pdf/10.1111/srt.12189.

[12] C. Magalhaes, R. Vardasca, M. Rebelo, R. Valenca-Filipe, M. Ribeiro, and J. Mendes, "Distinguishing melanocytic nevi from melanomas using static and dynamic infrared thermal imaging," *Journal of the European Academy of Dermatology and Venereology*, vol. 33, pp. 1700–1705, Sept. 2019.

[13] M. Bonmarin and F. A. Le Gal, "Lock-in thermal imaging for the early-stage detection of cutaneous melanoma: A feasibility study," *Computers in Biology and Medicine*, vol. 47, pp. 36–43, Apr. 2014.

[14] J. Verstockt, S. Verspeek, F. Thiessen, W. A. Tjalma, L. Brochez, and G. Steenackers, "Skin Cancer Detection Using Infrared Thermography: Measurement Setup, Procedure and Equipment," *Sensors*, vol. 22, p. 3327, Jan. 2022. Number: 9 Publisher: Multidisciplinary Digital Publishing Institute.

[15] J. Verstockt, F. E. F. Thiessen, I. Hoorens, L. Brochez, and G. Steenackers, "Comparative Analysis of Cooling Methods for Dynamic Infrared Thermography (DIRT)-Based Skin Cancer Diagnosis," *Applied Sciences*, vol. 13, p. 10105, Sept. 2023.